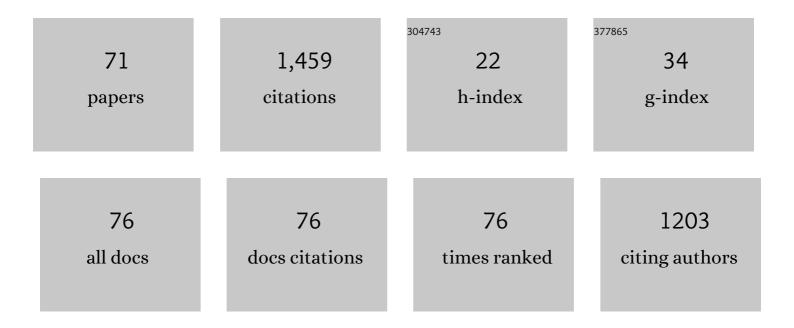
Lars Nielsen

List of Publications by Year in descending order

Source: https://exaly.com/author-pdf/8150276/publications.pdf Version: 2024-02-01



LADS NIFLSEN

#	Article	IF	CITATIONS
1	Monitoring Unsaturated Flow and Transport Using Crossâ€Borehole Geophysical Methods. Vadose Zone Journal, 2008, 7, 227-237.	2.2	112
2	Identifying Unsaturated Hydraulic Parameters Using an Integrated Data Fusion Approach on Crossâ€Borehole Geophysical Data. Vadose Zone Journal, 2008, 7, 238-248.	2.2	96
3	Internal architecture of a raised beach ridge system (Anholt, Denmark) resolved by ground-penetrating radar investigations. Sedimentary Geology, 2010, 223, 281-290.	2.1	68
4	Stratigraphy, Evolution, and Controls of A Holocene Transgressive–Regressive Barrier Island Under Changing Sea Level: Danish North Sea Coast. Journal of Sedimentary Research, 2015, 85, 820-844.	1.6	47
5	Integrated gravity and wide-angle seismic inversion fortwo-dimensional crustal modelling. Geophysical Journal International, 2000, 140, 222-232.	2.4	46
6	Visualizing Unsaturated Flow Phenomena Using Highâ€Resolution Reflection Ground Penetrating Radar. Vadose Zone Journal, 2011, 10, 84-97.	2.2	45
7	Seismic tomographic inversion of Russian PNE data along profile Kraton. Geophysical Research Letters, 1999, 26, 3413-3416.	4.0	42
8	Seaâ€level markers identified in groundâ€penetrating radar data collected across a modern beach ridge system in a microtidal regime. Terra Nova, 2009, 21, 474-479.	2.1	40
9	Implications of seismic scattering below the 8° discontinuity along PNE profile Kraton. Tectonophysics, 2002, 358, 135-150.	2.2	35
10	Full-waveform inversion of Crosshole GPR data: Implications for porosity estimation in chalk. Journal of Applied Geophysics, 2017, 140, 102-116.	2.1	34
11	Origin of upper-mantle seismic scattering - evidence from Russian peaceful nuclear explosion data. Geophysical Journal International, 2003, 154, 196-204.	2.4	33
12	Joint interpretation of beach-ridge architecture and coastal topography show the validity of sea-level markers observed in ground-penetrating radar data. Holocene, 2013, 23, 1238-1246.	1.7	33
13	Seismic and gravity modelling of crustal structure in the Central Graben, North Sea. Observations along MONA LISA profile 3. Tectonophysics, 2000, 328, 229-244.	2.2	31
14	Quantitative constraints on the sea-level fall that terminated the Littorina Sea Stage, southern Scandinavia. Quaternary Science Reviews, 2012, 40, 54-63.	3.0	30
15	Changes in Holocene relative sea-level and coastal morphology: A study of a raised beach ridge system on SamsÃ, southwest Scandinavia. Holocene, 2015, 25, 1402-1414.	1.7	30
16	The origin of teleseismicPnwaves: Multiple crustal scattering of upper mantle whispering gallery phases. Journal of Geophysical Research, 2003, 108, .	3.3	29
17	A Holocene relative sea-level database for the Baltic Sea. Quaternary Science Reviews, 2021, 266, 107071.	3.0	29
18	Morphology and sedimentary architecture of a beachâ€ridge system (<scp>A</scp> nholt, the) Tj ETQq0 0 0 rgB	T /Overlock 2.4	10 Tf 50 6

past â^1⁄41000 years. Boreas, 2012, 41, 422-434.

LARS NIELSEN

#	Article	IF	CITATIONS
19	Coastal lagoons and beach ridges as complementary sedimentary archives for the reconstruction of Holocene relative seaâ€level changes. Terra Nova, 2016, 28, 43-49.	2.1	25
20	Diffraction imaging of ground-penetrating radar data. Geophysics, 2019, 84, H1-H12.	2.6	25
21	Seismic scattering at the top of the mantle Transition Zone. Earth and Planetary Science Letters, 2003, 216, 259-269.	4.4	24
22	Mapping of the freshwater lens in a coastal aquifer on the Keta Barrier (Ghana) by transient electromagnetic soundings. Journal of Applied Geophysics, 2007, 62, 1-15.	2.1	24
23	Quantifying the influence of static-like errors in least-squares-based inversion and sequential simulation of cross-borehole ground penetrating radar data. Journal of Applied Geophysics, 2009, 68, 71-84.	2.1	24
24	Integrating ground-penetrating radar and borehole data from a Wadden Sea barrier island. Journal of Applied Geophysics, 2009, 68, 47-59.	2.1	24
25	Identification of crustal and upper mantle heterogeneity by modelling of controlled-source seismic data. Tectonophysics, 2006, 416, 209-228.	2.2	22
26	Accounting for Correlated Data Errors during Inversion of Crossâ€Borehole Ground Penetrating Radar Data. Vadose Zone Journal, 2008, 7, 263-271.	2.2	22
27	Sedimentary architecture and depositional controls of a Holocene waveâ€dominated barrierâ€island system. Sedimentology, 2018, 65, 1170-1212.	3.1	22
28	Luminescence dating of buried cobble surfaces from sandy beach ridges: a case study from Denmark. Boreas, 2019, 48, 841-855.	2.4	22
29	Bayesian Markovâ€Chainâ€Monteâ€Carlo Inversion of Timeâ€Lapse Crosshole GPR Data to Characterize the Vadose Zone at the Arrenaes Site, Denmark. Vadose Zone Journal, 2012, 11, vzj2011.0153.	2.2	21
30	Inferring the Subsurface Structural Covariance Model Using Crossâ€Borehole Ground Penetrating Radar Tomography. Vadose Zone Journal, 2008, 7, 249-262.	2.2	20
31	Integrated seismic analysis of the Chalk Group in eastern Denmark—Implications for estimates of maximum palaeo-burial in southwest Scandinavia. Tectonophysics, 2011, 511, 14-26.	2.2	20
32	Morphological records of storm floods exemplified by the impact of the 1872 Baltic storm on a sandy spit system in southâ€eastern Denmark. Earth Surface Processes and Landforms, 2014, 39, 499-508.	2.5	20
33	Sea-level proxies in Holocene raised beach ridge deposits (Greenland) revealed by ground-penetrating radar. Scientific Reports, 2017, 7, 46460.	3.3	20
34	Seismic velocity structure of a large mafic intrusion in the crust of central Denmark from project ESTRID. Tectonophysics, 2006, 420, 105-122.	2.2	19
35	Mapping sand layers in clayey till using crosshole ground-penetrating radar. Geophysics, 2018, 83, A21-A26.	2.6	18
36	Geostatistical inference using crosshole ground-penetrating radar. Geophysics, 2010, 75, J29-J41.	2.6	17

LARS NIELSEN

#	Article	IF	CITATIONS
37	TeleseismicPnarrivals: influence of mantle velocity gradient and crustal scattering. Geophysical Journal International, 2003, 152, F1-F7.	2.4	16
38	Constraints on reflective bodies below the 8° discontinuity from reflectivity modelling. Geophysical Journal International, 2001, 145, 759-770.	2.4	15
39	Ground-penetrating radar imaging of carbonate mound structures and implications for interpretation of marine seismic data. AAPG Bulletin, 2004, 88, 1069-1082.	1.5	15
40	Comparing Plume Characteristics Inferred from Crossâ€Borehole Geophysical Data. Vadose Zone Journal, 2012, 11, vzj2012.0031.	2.2	14
41	Estimation of Recharge from Longâ€īerm Monitoring of Saline Tracer Transport Using Electrical Resistivity Tomography. Vadose Zone Journal, 2015, 14, 1-13.	2.2	14
42	Layered crust–mantle transition zone below a large crustal intrusion in the Norwegian–Danish Basin. Tectonophysics, 2009, 472, 194-212.	2.2	13
43	23. Estimation of Chalk Heterogeneity from Stochastic Modeling Conditioned by Crosshole GPR Traveltimes and Log Data. , 2010, , 379-396.		13
44	High-resolution shear-wave seismics across the Carlsberg Fault zone south of Copenhagen — Implications for linking Mesozoic and late Pleistocene structures. Tectonophysics, 2016, 682, 56-64.	2.2	12
45	Optical dating of cobble surfaces determines the chronology of Holocene beach ridges in Greenland. Boreas, 2021, 50, 606-618.	2.4	12
46	Continuous record of Holocene sea-level changes and coastal development of the Kattegat island LæsÃ, (4900 years BP to present). Bulletin of the Geological Society of Denmark, 2016, 64, 1-55.	1.1	12
47	Seismic tomographic interpretation of Paleozoic sedimentary sequences in the southeastern North Sea. Geophysics, 2005, 70, R45-R56.	2.6	11
48	Examining the information content of time-lapse crosshole GPR data collected under different infiltration conditions to estimate unsaturated soil hydraulic properties. Advances in Water Resources, 2013, 54, 38-56.	3.8	10
49	Location of the Carlsberg Fault zone from seismic controlled-source fan recordings. Geophysical Research Letters, 2004, 31, n/a-n/a.	4.0	9
50	Threeâ€dimensional architecture and development of Danian bryozoan mounds at Limhamn, southâ€west Sweden, using groundâ€penetrating radar. Sedimentology, 2009, 56, 695-708.	3.1	9
51	Early diagenetic evolution of Chalk in eastern Denmark. Depositional Record, 2016, 2, 154-172.	1.7	9
52	Deep onshore reflection seismic imaging of the chalk group strata using a 45Âkg accelerated weight-drop and combined recording systems with dense receiver spacing. Geophysics, 2019, 84, B259-B268.	2.6	9
53	Seismic evidence for deep Palaeozoic sedimentary units in the RingkÃ,bing-Fyn High offshore Denmark. Bulletin of the Geological Society of Denmark, 1998, 45, 1-10.	1.1	9
54	Integrated seismic interpretation of the Carlsberg Fault zone, Copenhagen, Denmark. Geophysical Journal International, 2005, 162, 461-478.	2.4	8

LARS NIELSEN

#	Article	IF	CITATIONS
55	Coastal evolution of a cuspate foreland (Flakket, Anholt, Denmark) between 2006 and 2010 Bulletin of the Geological Society of Denmark, 2011, 59, 37-44.	1.1	8
56	Pitfalls in velocity analysis for strongly contrasting, layered media – Example from the Chalk Group, North Sea. Journal of Applied Geophysics, 2018, 149, 52-62.	2.1	7
57	Simultaneous estimation of lithospheric uplift rates and absolute sea level change in southwest Scandinavia from inversion of sea level data. Geophysical Journal International, 2014, 199, 1018-1029.	2.4	6
58	On the usage of diffractions in ground-penetrating radar reflection data: Implications for time-lapse gas migration monitoring. Geophysics, 2020, 85, H83-H95.	2.6	6
59	Rock-physics characterization of chalk by combining acoustic and electromagnetic properties. Geophysics, 2022, 87, MR1-MR11.	2.6	6
60	Upscaling of outcrop information for improved reservoir modelling – exemplified by a case study on chalk. Petroleum Geoscience, 2021, 27, .	1.5	4
61	Practical data acquisition strategy for time-lapse experiments using crosshole GPR and full-waveform inversion. Journal of Applied Geophysics, 2021, 191, 104362.	2.1	4
62	Beach-ridge architecture constrained by beach topography and ground-penetrating radar, Itilleq (Laksebugt), south-west Disko, Greenland – implications for sea-level reconstructions Bulletin of the Geological Society of Denmark, 2018, 66, 167-179.	1.1	3
63	GENERATING RADAR-WAVE VELOCITY FIELD FOR DEPTH CONVERSION USING INFORMATION ON GROUNDWATER LEVEL. , 2013, , .		2
64	Improved seismic interpretation of a salt diapir by utilization of diffractions, exemplified by 2D reflection seismics, Danish sector of the North Sea. Interpretation, 2020, 8, T77-T88.	1.1	2
65	Geophysics for urban mining and the first surveys in Denmark: rationale, field activity and preliminary results. Geological Survey of Denmark and Greenland Bulletin, 0, , .	2.0	2
66	Quantitative seismic interpretation of the Lower Cretaceous reservoirs in the Valdemar Field, Danish North Sea. Petroleum Geoscience, 2021, 27, .	1.5	1
67	Seismic interpretation pitfalls caused by interference effects, exemplified by seismic modeling of outcropping chalk successions. Interpretation, 0, , 1-31.	1.1	1
68	Full-waveform inversion of cross-hole GPR data collected in a strongly heterogeneous chalk reservoir analogue with sharp permittivity and conductivity contrasts. , 2014, , .		0
69	MORPHODYNAMICS OF AN ABANDONED DELTA LOBE IN NE GREENLAND. , 2019, , .		0
70	Rock physics templates for chalk by combining acoustic and EM velocity. , 2019, , .		0
71	Data-driven source wavelets for crosshole ground-penetrating radar full-waveform modeling. , 2020,		Ο